Acylation of SC4 dodecapeptide increases bactericidal potency against Gram-positive bacteria, including drug-resistant strains

Nathan A. LOCKWOOD*†, Judith R. HASEMAN*, Matthew V. TIRRELL‡ and Kevin H. MAYO*[1]

*Department of Biochemistry, Molecular Biology and Biophysics, University of Minnesota, Minneapolis, MN 55455, U.S.A., †Department of Chemical Engineering and Materials Science, University of Minnesota, Minneapolis, MN 55455, U.S.A., and ‡Departments of Chemical Engineering and Materials, University of California Santa Barbara, Santa Barbara, CA 93106, U.S.A.

We have conjugated dodecyl and octadecyl fatty acids to the N-terminus of SC4, a potently bactericidal, helix-forming peptide 12-mer (KLFKRHLKWKII), and examined the bactericidal activities of the resultant SC4 'peptide-amphiphile' molecules. SC4 peptide-amphiphiles showed up to a 30-fold increase in bactericidal activity against Gram-positive strains (*Staphylococcus aureus*, *Streptococcus pyogenes* and *Bacillus anthracis*), including *S. aureus* strains resistant to conventional antibiotics, but little or no increase in bactericidal activity against Gram-negative bacteria (*Escherichia coli* and *Pseudomonas aeruginosa*). Fatty acid conjugation improved endotoxin (lipopolysaccharide) neutralization by 3- to 6-fold. Although acylation somewhat increased lysis of human erythrocytes, it did not increase lysis of endothelial cells, and the haemolytic effects occurred at concentrations 10- to 100-fold higher than those required for bacterial cell lysis. For insight into the mechanism of action of SC4 peptide-amphiphiles, CD, NMR and fluorescence spectroscopy studies were performed in micelle and liposome models of eukaryotic and bacterial cell membranes. CD indicated that SC4 peptide-amphiphiles had the strongest helical tendencies in liposomes mimicking bacterial membranes, and strong membrane integration of the SC4 peptide-amphiphiles was observed using tryptophan fluorescence spectroscopy under these conditions; results that correlated with the increased bactericidal activities of SC4 peptide-amphiphiles. NMR structural analysis in micelles demonstrated that the two-thirds of the peptide closest to the fatty acid tail exhibited a helical conformation, with the positively-charged side of the amphipathic helix interacting more with the model membrane surface. These results indicate that conjugation of a fatty acid chain to the SC4 peptide enhances membrane interactions, stabilizes helical structure in the membrane-bound state and increases bactericidal potency.

Key words: antibacterial peptide, CD, fatty acid, NMR, peptide-amphiphile.

INTRODUCTION

Antibacterial peptides are found in the innate defence systems of organisms ranging from insects [1] to amphibians [2] to mammals [3]. The prevalence of antibacterial peptides in natural defence systems and their novel mode of action, in which bacteria are killed by membrane disruption rather than inhibition of specific metabolic pathways, has led to significant work toward antimicrobial peptide agents that could circumvent the problem of bacterial drug resistance. A comprehensive database of antimicrobial peptides maintained at the University of Trieste, Italy, contains over 800 peptide sequences [4], and databases of related peptides include hundreds of other sequences [5,6]. Examples of bactericidal peptides include α-helical magainins [7], β-sheet defensins [8], proline/arginine-rich PR39 [9] and tryptophan-rich indolicidin [10]. Although most antibacterial peptides are active without post-translational modification, polymyxins and lipopeptaibols have a short, N-terminally-linked fatty acid that appears to be crucial for bactericidal activity [11,12].

Antibacterial peptides of disparate lengths, sequences and secondary structures have two distinguishing features: a net positive charge, typically $+2$ to $+6$, and an overall amphipathic fold, imparting polar and hydrophobic faces to the molecule [13]. The cationic nature of antibacterial peptides promotes selective interaction with the negatively-charged surface of bacterial membranes over the neutral surface of eukaryotic membranes [14], whereas the amphipathic conformation of the peptide promotes bacterial cell lysis [15].

Recently, several investigators have produced fatty acid conjugates of antibacterial peptides in order to improve bactericidal activity, borrowing in principle from the naturally occurring polymyxins and lipopeptaibols. In these investigations, N-terminal fatty acid conjugates increased bactericidal activity of cathepsin G [16,17] and lactoferrin peptides [18,19]. Antibiotic activity was similarly increased in magainin [20] and cecropin-melittin [21] peptides by fatty acid conjugation. Fatty acid- and lipid-conjugated peptides have also been developed in our labortory as 'peptide-amphiphiles' for a variety of applications [22]. Peptide-amphiphiles self-assemble in solution [23], and preserve biological function and secondary structure in the peptide headgroup [24].

Similarities between peptide-amphiphiles and naturally occurring and synthetic lipopeptide antimicrobials led us to combine peptide-amphiphile technology with a potent antibacterial peptide 12-mer, SC4 [25]. SC4 displays bactericidal activity at nanomolar concentrations against Gram-negative bacteria and at submicromolar concentrations against Gram-positive bacteria. The peptide also effectively neutralizes LPS (lipopolysaccharide)

Abbreviations used: CFU, colony-forming units; DPC, dodecylphosphatidylcholine; DPPC, 1,2-dipalmitoyl-*sn*-glycero-3-phosphocholine; DPPE, 1,2-dipalmitoyl-*sn*-glycero-3-phosphoethanolamine; DPPG, 1,2-dipalmitoyl-*sn*-glycero-3-[phospho-*rac*-(1-glycerol)]; LPS, lipopolysaccharide; NOE, nuclear Overhauser effect; TFA, trifluoroacetic acid.

[1] To whom correspondence should be addressed (mayox001@umn.edu).

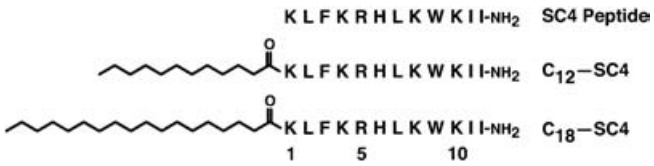

Figure 1 Peptide sequences, peptide-amphiphile structures and nomenclature used in the present study

The '-NH_2' at the right of each sequence indicates amidation of the C-terminus.

endotoxin and shows no haemolytic activity below 100 μM. SC4 folds as an amphipathic helix in membrane-mimicking trifluoroethanol/water solutions and appears to exert bactericidal effects through a membrane-permeabilizing mechanism similar to that reported for other bactericidal peptides in this class of antibacterial agents [26].

In the present study, we have conjugated the N-terminus of the SC4 antibacterial peptide to fatty acid chains and assessed the bactericidal activity and probed the bactericidal mechanism of the resultant SC4 peptide-amphiphiles. To determine the spectrum of bactericidal activity, several clinically-relevant bacterial strains were investigated: Gram-negative *Escherichia coli* and *Pseudomonas aeruginosa*; Gram-positive *Staphylococcus aureus*, *Streptococcus pyogenes* and *Bacillus anthracis*; and two drug-resistant strains of *S. aureus*. We also investigated the lytic activity of the SC4 peptide-amphiphiles against human erythrocytes and endothelial cells as a measure of potential toxicity and as an indicator of bacterial membrane specificity. For insight into the bactericidal mechanism, we employed NMR, CD and tryptophan fluorescence spectroscopies to assess the secondary structure and membrane interactions of the SC4 peptide-amphiphiles in the presence of micelles and liposomes which mimic bacterial and eukaryotic membranes.

EXPERIMENTAL

Peptide sequences and amphiphile structure

The designed 12-residue SC4 peptide sequence was based on a peptide derived from bactericidal/permeability-increasing protein [25]. C12 and C18 amphiphile versions of SC4 have the appropriate fatty acid covalently linked to the N-terminus of the peptide (Figure 1). The SC4 peptide and the SC4 peptide-amphiphiles were amidated at the C-terminus.

SC4 peptide synthesis

The SC4 peptide was synthesized at the Microchemical Facility, University of Minnesota, on a Milligen/Biosearch 9600 peptide solid-phase synthesizer using fluoren-9-ylmethoxycarbonyl (Fmoc) chemistry. Freeze-dried crude peptide was purified by preparative reversed-phase HPLC on a C18 column with an elution gradient of 0–60 % acetonitrile with 0.1 % TFA (trifluoroacetic acid) in water. Purity and composition of the peptide was verified by HPLC, amino-acid analysis and matrix-assisted laser-desorption ionization–time-of-flight MS.

SC4 peptide-amphiphile synthesis

Peptide-amphiphiles were synthesized from resin-bound SC4 peptide and dodecanoic (lauric) or octadecanoic (stearic) fatty acids with manual fluoren-9-ylmethoxycarbonyl solid-phase chemistry essentially as described previously [22]. Briefly, the C12 or C18 fatty acid tails were N-terminally coupled to the resin-bound peptide for 3 h with 4-fold molar excess of 2-(1*H*-benzotriazole-1-yl)-1,1,3,3-tetramethyluronium hexafluorophosphate (HBTU), 1-hydroxybenzotriazole (HOBt), *N*,*N*-di-isopropylethylamine (DIEA) and fatty acid tails in dichloromethane (DCM)/*N*,*N*-dimethylformamide (DMF). Peptide-amphiphiles and protecting groups were cleaved from the resin by treatment with Reagent K (82.5 % TFA/5 % phenol/5 % water/5 % thioanisole/2.5 % ethanedithiol) for 2 h. Crude peptide-amphiphiles were purified by HPLC on a reversed-phase C4 column with a gradient of 30–60 % (for C12-SC4) or 35–70 % (for C18-SC4) acetonitrile in water with 0.1 % TFA. The identity of the purified peptide-amphiphile products was verified by matrix-assisted laser-desorption ionization–time-of-flight MS.

Bacterial strains

Gram-negative *E. coli* J96 and IA2 are smooth strain, uropathogenic clinical isolates described by Johnson and Brown [27] and were a gift from J. R. Johnson (Department of Microbiology, University of Minnesota, Minneapolis, MN, U.S.A.). *P. aeruginosa* type I is a clinical smooth-strain isolate. Gram-positive MN8 (described by Bohach et al. [28]) and MNHO (described by Schlievert and Blomster [29]) are patient isolates of *S. aureus*; Eaton and Wilson are two patient isolates of *Streptococcus pyogenes*. M497880 and W73134 are clinical isolate strains of *S. aureus* that display resistance to all conventional antibiotics except vancomycin. *B. anthracis* is a laboratory strain from P. M. Schlievert (Department of Microbiology, University of Minnesota, Minneapolis, MN, U.S.A.). All Gram-positive strains were provided by P. M. Schlievert. *E. coli* and *S. aureus* strains were maintained and plated on nutrient agar plates. *Streptococcus pyogenes* strains were maintained on blood agar plates and plated on brain–heart infusion agar plates. *B. anthracis* was grown in Todd–Hewitt broth.

Bactericidal assay

Pyrogen-free solutions were used throughout the assay. Bacteria at log-phase growth were obtained by transferring an overnight culture or scraping crystals from −85 °C glycerol stocks of overnight cultures. Bacteria were washed and resuspended in 0.9 % sodium chloride solution with adjustment to a D_{650} that yielded 3×10^8 CFU (colony-forming units)/ml. Bacteria were then diluted 1:10 in 0.08 M citrate phosphate buffer, pH 7.0 (prepared by mixing 0.08 M citric acid with 0.08 M dibasic sodium phosphate). Bacterial samples (0.15 ml) were combined with the appropriate amount of peptide and 1.0 ml of buffer in 17 mm (diameter) × 100 mm (length) polypropylene tubes and incubated in a reciprocal water bath shaker at 37 °C for 30 min. For all bacterial strains except *B. anthracis*, 1:10, 1:100, and 1:1000 dilutions were then prepared in 0.9 % sodium chloride solution and 20 μl of each dilution was streaked across an agar plate. Gram-negative organisms were plated on nutrient agar plates containing 2 % agar and Gram-positive organisms were plated on MacConkey agar (2 %). Plates were incubated overnight at 37 °C and colonies counted the next morning. The dilution containing 10–100 bacterial colonies was counted and the number multiplied by 50 to adjust all counts to the number of bacteria killed/ml. For *B. anthracis*, 5 ml of Todd–Hewitt broth was added to the solutions following incubation, and bacteria were grown to mid-log phase under continuous shaking. For *B. anthracis*, cell survival was assayed by measuring D_{650}.

Bactericidal activities are reported as LD_{50} values determined by fits of the data to the sigmoidal dose–response equation:

$$\text{Bacteria killed (\%)} = R_{min} + \{(R_{min} - R_{max})/[1 + (C/LD_{50})\hat{}m]\}$$

where C is the concentration; $R_{min} = 0$, the minimum response; $R_{max} = 100$, the maximum response; LD_{50} is the midpoint of the transition; and m is the slope of the transition. LD_{50} and m were the free variables used to fit the data. Although the minimal inhibitory concentration (MIC) is conventionally used to express bactericidal activity, LD_{50} values were used here to discriminate better between the effectiveness of these compounds against different bacterial strains. An estimate of the minimal inhibitory concentration value can be derived from dose–response curves at the value which kills 100 % of the bacteria.

Limulus amoebocyte lysate assay for LPS neutralization

The ability of SC4 peptide and amphiphiles to neutralize endotoxin was measured using the chromogenic QCL-1000 kit from BioWhittaker (Walkersville, MD, U.S.A.). This method is quantitative for Gram-negative bacterial endotoxin (LPS) and uses peptide inhibition of LPS-mediated activation of a proenzyme as a measure of activity [31]. Peptides of the appropriate concentration were mixed with *Limulus* amoebocyte lysate, 0.04 unit (0.01 ng) of *E. coli* 055:B5 LPS (Sigma), and a colourless synthetic substrate (acetyl-Ile-Glu-Ala-Arg-*p*-nitroaniline). Peptide binding to LPS was determined by monitoring enzymic conversion of the substrate to yellow *p*-nitroaniline at A_{410}. Endotoxin concentration was determined from the initial rate of enzyme activation. IC_{50} values for LPS binding were determined by fitting to a dose–response curve.

Eukaryotic cell lysis activity

The lytic activity of SC4 molecules against human erythrocytes and human endothelial cells was measured. Erythrocytes were washed three times with PBS (35 mM phosphate buffer/0.15 M NaCl, pH 7.0) prior to performing the haemolysis assay. Serially-diluted peptides (1–100 μM; volume, 100 μl) in PBS were added to Eppendorf tubes containing 100 μl of 0.4 % (v/v) human erythrocytes suspended in PBS. Tubes were incubated for 1 h at 37 °C and then centrifuged at 1000 ***g*** for 5 min. Aliquots (100 μl) of the supernatant were then transferred to Eppendorf tubes and haemolysis was measured at A_{414}. Zero and 100 % haemolysis were determined in PBS and 1 % Triton X-100 respectively. The percentage of haemolysis was calculated as:

$$\text{Haemolysis (\%)} = \{[A_{414}(\text{peptide}) - A_{414}(\text{PBS})]/ [A_{414}(\text{Triton X-100}) - A_{414}(\text{PBS})]\} \times 100$$

Bacterial and eukaryotic cell membrane mimics

Bilayer-forming phospholipids and micelle-forming detergents were used as membrane mimics. Liposomes formed from zwitterionic DPPC (1,2-dipalmitoyl-*sn*-glycero-3-phosphocholine) were used as a mimic of eukaryotic membranes, which comprise predominantly neutral zwitterionic lipids. Liposomes comprising 7:3 molar mixture of neutral DPPE (1,2-dipalmitoyl-*sn*-glycero-3-phosphoethanolamine) and negatively-charged DPPG {1,2-dipalmitoyl-*sn*-glycero-3-[phospho-*rac*-(1-glycerol)]}were used to mimic bacterial membranes, which have an overall negative membrane charge and a composition essentially matching that used in the mimic. Micelle-forming DPC (dodecylphosphatidylcholine) and SDS were used as simple mimics of eukaryotic and bacterial membranes respectively in NMR experiments, which require small aggregate size to limit resonance broadening, and in CD experiments in order to minimize light scattering from aggregates.

Liposome preparation

DPPC, DPPE, and DPPG phospholipids were obtained from Avanti Polar Lipids. Chloroform solutions of pure phospholipid were mixed in a glass tube at desired lipid ratios and dried under a low flow of N_2 to form a thin lipid film. Residual solvent was removed under vacuum for several hours. The resulting lipid film was hydrated for at least 1.5 h at temperatures above the lipid transition temperature with an appropriate volume of water to yield a final lipid concentration of 4 mM. The solutions were periodically vortexed during the hydration period. Solutions were then sonicated for 20 min or more in a bath sonicator at temperatures above the lipid transition temperature to produce small unilamellar liposomes. Lipid solutions were cooled to 22 °C prior to use.

Liposome and micelle solution preparation

Aqueous stock solutions were prepared by dissolving dry peptide, amphiphile or detergent in water; aqueous lipid stock solutions were prepared as described above. SDS or DPC detergent/peptide solutions were prepared by separately diluting stock solutions of peptide-amphiphile and detergent with water to give twice the desired final concentrations. The diluted solutions were mixed to give the appropriate final peptide concentration (0.1 mM for CD and 0.5 mM for NMR) at a peptide/detergent ratio of 1:50 (DPC) or 1:100 (SDS). These ratios correspond to roughly one peptide per micelle, based on the aggregation numbers of the detergents. Detergent micelle solutions for fluorescence spectroscopy were prepared as above, but with a final peptide concentration of 5–10 μM and a peptide/detergent ratio of 1:500 in DPC and 1:1000 in SDS. Liposome solutions were prepared similarly, mixing diluted stocks of peptide and liposomes to give a final peptide concentration of 5–10 μM at a peptide/lipid ratio of 1:20. The method of mixing dilute solutions of peptide and detergent/lipid limited the aggregation observed when mixing stocks of higher concentration.

CD

CD spectra were recorded on a Jasco J-710 spectrophotometer at 25 °C or 37 °C in a 0.1 cm (aqueous and detergent solutions) or 1.0 cm (lipid solutions) path-length quartz cuvette. Acquisition was performed with a 50 nm/min scan rate, 1 nm bandwidth and 2 s response. The corresponding baseline (water, detergent or lipid solution) was subtracted from each spectrum. Reported spectra are averages of 6 scans and are expressed as $[\theta]_{m.r.w.}$. Peptide concentrations were 0.1 mM in water or detergent micelle solutions, 10 μM in liposome solutions. CD basis spectra were measured with polylysine and poly(glutamic acid) (Sigma) with conditions and parameters reported previously [32,33]. Linear combinations of α-helix, β-sheet and random-coil basis spectra were used to fit experimental CD spectra for estimation of secondary structure contributions.

NMR measurements

Solutions for NMR measurements were prepared as described above, but dissolved in 90 % water/10 % ^2H_2O to give a final

peptide/amphiphile concentration of 0.5 mM, pH 5.3 (unbuffered). Proton NMR spectra were acquired on a Varian UNITY Plus-600 NMR spectrometer at 25 °C. Spin systems were identified with 2D-homonuclear magnetization transfer (TOCSY) spectra obtained with a mixing time of 60 ms. NOESY experiments with a mixing time of 100 ms were performed for conformational analysis. The water resonance was suppressed with WATERGATE (TOCSY) or WET (NOESY) pulse sequences. For structural analysis experiments, 2D-NMR spectra were collected for 512 t1 increments, each with 1k complex data points over a spectral width of 8 kHz in both dimensions with the carrier placed on the water resonance; 32 scans were averaged for each t1 increment. Data were processed offline with NMRPipe [34] and Sparky (provided by T. D. Goddard, and D. G. Kneller, University of California, San Francisco, CA, U.S.A.) on an Apple iBook. Data sets were multiplied in both dimensions by a shifted sine-bell function, baseline-corrected, and zero-filled to 1k in the t1 dimension and 2k in the t2 dimension prior to Fourier transformation. Shorter TOCSY experiments (4 transients for each of 128 t1 increments) were used to investigate peptide–micelle interactions and for examining hydrogen-bonding through the temperature dependence of NH chemical shifts.

Structural modelling

Inter-proton distance constraints were derived from NOE (nuclear Overhauser effect) cross-peaks assigned in ^{1}H NOESY spectra. NOEs were classified as strong, medium, weak or very weak corresponding to upper-bound distance constraints of 2.9, 3.3, 4.0 and 5.0 Å respectively. The lower-bound constraint between non-bonded protons was set to 1.8 Å. A 0.5 Å correction was added to the upper bound for NOEs involving side-chain protons. Hydrogen-bond constraints were identified from the pattern of sequential NOEs involving NH and C_α H protons, and NH temperature coefficients ($d\delta/dT$), which fell into two groups: > 0.004 p.p.m./K (K1, L2, W9, K10) and < 0.004 p.p.m./K (F3, K4, R5, H6, L7, K9, I12, I13). Each hydrogen bond was defined by upper-bound distance constraints of 3.5 Å and 4.0 Å for NH–O and N–O distances respectively.

The X-PLOR software package [35] was used with NOE-derived distance constraints to calculate structures of C12-SC4 in DPC micelles, as described previously [25]. Final structures were obtained by filtering the results such that none of the final structures had NOE violations greater than 0.5 Å, and the bond angles, lengths or improper angles did not deviate from ideal geometry more than 5°, 0.05 Å and 5° respectively. Structures were superimposed and visualized with the VMD software package [36] and analysed with X-PLOR routines.

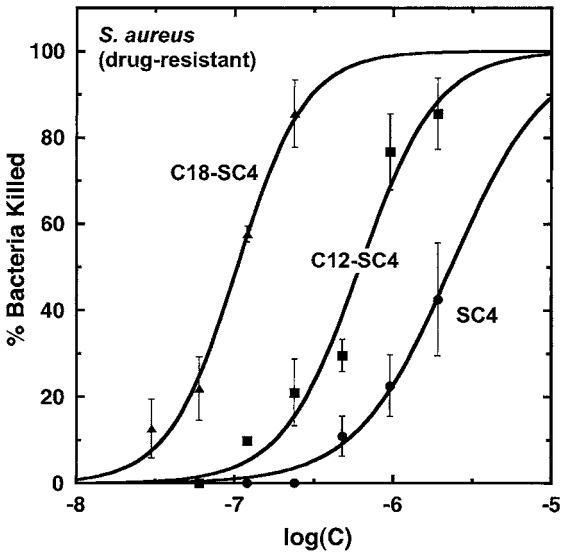

Figure 2 Examples of dose–response curves for SC4 (●), C12-SC4 (■) and C18-SC4 (▲) against drug-resistant, Gram-positive *S. aureus* W73134 bacteria

Lines are sigmoidal curve fits used to determine LD_{50} values.

Tryptophan fluorescence spectroscopy

Tryptophan fluorescence spectra were obtained at 25 or 37 °C on an ISS-K2 steady-state fluorometer. Solutions were prepared as described above and placed in a 1-cm quartz cuvette for measurement. Peptide concentration was 5 μM in water or 1:20 (mol/mol) in lipid solutions. Samples were excited at 280 nm and a single emission spectrum recorded from 300–450 nm with a 1 nm step size and 1 s integration time.

RESULTS

Bactericidal activity

SC4 peptide, and C12-SC4 and C18-SC4 peptide-amphiphiles (Figure 1) were tested for bactericidal activity against several clinically-relevant strains of Gram-negative, Gram-positive and drug-resistant bacteria. Activities are reported as LD_{50} values, as determined by sigmoidal fits of dose–response data (exemplified in Figure 2). Both C12-SC4 and C18-SC4 generally showed increased bactericidal activity relative to SC4 (Table 1). The maximal increase in bactericidal activity as a result of fatty acid

Table 1 Biological activities of SC4 peptide and amphiphiles

All strains are clinical isolates.

	Bactericidal activity (LD_{50}, μM)											
	E. coli			*Staph. aureus*				*Strep. pyogenes*				
Peptide	J96	IA2	*P. aeruginosa* Type I	MN8	MNHO	M49780*	W73134*	Eaton	Wilson	*B. anthracis*	LPS Binding (IC_{50}, μM)	Haemolysis (LD_{50}, μM)
SC4	0.12	0.21	0.028	1.3	2.3	2.0	2.3	> 2.0	> 1.0	> 15	0.59	> 375
C12-SC4	0.08	0.08	0.035	0.7	0.34	0.66	0.62	0.066	0.16	3.25	0.23	6.2
C18-SC4	0.23	0.19	0.042	0.1	0.068	0.24	0.10	0.11	0.13	2.23	0.082	1.9

* Strains show resistance to all conventional antibiotics, except vancomycin.

conjugation was greater than 30-fold against *S. aureus* and drug-resistant *S. aureus* strains. Even though the effective increase against *Streptococcus pyogenes* could not be calculated accurately due to lack of activity from SC4, the increase was greater than 20-fold using the maximum concentration of SC4 tested (2.0 mM). When compared with SC4, C12-SC4 and C18-SC4 showed little, if any, increased activity against Gram-negative strains, with LD_{50} values varying by a factor of two or less against *E. coli* and remaining essentially unchanged against *P. aeruginosa*. The LD_{50} values for SC4 (Table 1) vary from those reported by Mayo et al. [25], which is due primarily to biological variance. In any event, these current SC4 LD_{50} values were used as controls for observing the relative effects of acylation on bactericidal activity.

LPS neutralization

Lysis of Gram-negative bacteria produces the endotoxin LPS, which, when released in the body in high enough amounts, can trigger the pathological disorder endotoxaemia and lead to sepsis. In this respect, peptides that are both bactericidal and effectively neutralize LPS are of considerable pharmaceutical importance. We therefore measured the LPS binding and neutralizing activities of SC4, C12-SC4 and C18-SC4 with the *Limulus* amoebocyte assay. IC_{50} values were determined from dose–response curves. C12-SC4 and C18-SC4 showed LPS-binding activities approx. 3-fold and 6-fold higher than the SC4 peptide respectively (Table 1). Peptides with higher hydrophobicity tend to bind LPS more strongly, and the hydrophobic nature of the tail groups in SC4 amphiphiles makes binding to the lipid A portion of LPS the most likely site for interaction and subsequent neutralization.

Eukaryotic cell lysis activity

Because SC4 and its amphiphiles probably disintegrate bacterial cell membranes, we assessed their ability to lyse eukaryotic cells. If administered as an antibiotic in animals, the two main eukaryotic cell types that these agents would encounter in blood vessels are erythrocytes and the endothelial cells lining the vessel walls. At concentrations up to 0.4 mM, SC4, C12-SC4 or C18-SC4 did not lyse endothelial cells in culture (results not shown). SC4 also demonstrated little haemolytic activity, up to 0.4 mM. However, both C12-SC4 and C18-SC4 lysed erythrocytes in the micromolar range (Table 1); C18-SC4 was roughly 3-fold more haemolytic than C12-SC4.

CD

For insight into the structural behaviour of SC4 peptide-amphiphiles interacting with membranes, we examined the conformation of SC4, C12-SC4 and C18-SC4 in aqueous solution and in the presence of eukaryotic membrane mimics (DPC micelles or DPPC liposomes) and bacterial membrane mimics (SDS micelles or DPPE/DPPG liposomes) by CD spectroscopy (Figure 3). Aqueous solutions of pure SC4, C12-SC4 and C18-SC4 gave CD spectra consistent with disordered structures (results not shown); fits of the data using a linear combination of basis spectra indicated 63 % to 77 % random coil for each of the molecules. Similar CD spectra were observed for SC4 in either DPC or SDS micellar environments, with fits indicating 62–67 % coil. However, CD spectra of C12-SC4 and C18-SC4 indicated 78 % and 82 % α-helix in DPC micelles respectively, and 53 % and 54 % α-helix in SDS micelles respectively.

In eukaryotic membrane-mimicking DPPC liposomes, none of the SC4 molecules showed significant helical structure (76 % coil for SC4 and 60 % coil for C12- and C18-SC4). In bacterial membrane-mimicking DPPE/DPPG (70 % DPPE/30 % DPPG) liposomes, the quality of CD spectra was relatively poor due to formation of hazy solutions when SC4 or its amphiphiles were mixed with DPPE/DPPG liposome solutions. This effect was minimized, although not eliminated, by using solutions of lower peptide and lipid concentrations. SC4 spectra were particularly noisy and could not be readily interpreted other than to say that above 215 nm the spectrum looked similar to that in DPPC. CD spectra of C12-SC4 and C18-SC4 were distinct from their corresponding DPPC spectra. Both C12-SC4 and C18-SC4 in DPPE/DPPG gave CD spectra consistent with structured peptides. Qualitatively, the overall shape of these CD traces suggests the presence of significant α-helix conformation.

NMR studies

We chose to perform NMR studies on C12-SC4 peptide-amphiphiles in SDS and DPC micellar environments as a result of the overall improved solution behaviour and the smaller aggregate size than in liposome systems. TOCSY and NOESY spectra of C12-SC4 in DPC showed well-resolved and well-dispersed cross-peaks in the αH-NH and NH-NH regions (Figure 4), indicative of the presence of stable peptide conformation. Spectra of C12-SC4 in SDS showed similar dispersion, but fewer NOE cross-peaks. C12-SC4 αH and NH resonances are generally shifted upfield relative to SC4 in the same micellar solutions, particularly αH resonances belonging to residues Lys-1 through His-7 and NH resonances belonging to residues Leu-2 through Lys-8 (Figure 5). The 'shift difference' used here compares the C12-SC4 amphiphile with the SC4 peptide under the same conditions. This differs from the standard use of the chemical shift index, which compares shifts with a random-coil state [37]. The nature of these shifts suggests that the presence of the acyl chain in C12-SC4, on interacting with these micellar systems, has induced a more stable helix within this N-terminal region of the peptide [37]. It should be noted, however, that Phe-4 and Trp-9 aromatics may induce ring current shifting of various resonances to attenuate actual upfield shifts of some αH or NH resonances; this may help explain why some αH and NH shift differences were either zero or positive. αH and NH shift differences are generally greater for the peptide-amphiphile in DPC than in SDS, which suggests increased helix stability of C12-SC4 in DPC. NOESY data support this conclusion in that long-range NOEs are both more numerous and more intense for C12-SC4 in the presence of DPC micelles than in SDS micelles.

NMR conformational modelling

In order to characterize the conformation of the SC4 amphiphiles in more detail, we performed a full NMR structure analysis on C12-SC4 in DPC micelles at 25 °C, conditions that showed the highest level of α-helical content in our CD analysis. The pattern of NOEs observed for C12-SC4 in DPC micelles was consistent with α-helical conformation in residues 1–9 (Figure 6); the patterns for C12-SC4 in SDS micelles were weaker but consistent with a similar helical conformation.

Conformational modelling was performed for C12-SC4 in DPC micelles using NOE distance restraints obtained from NOESY experiments. A total of 196 NOE distance constraints were derived from analysis of NOESY spectra, including 23 intraresidue, 83 sequential and 90 medium-range ($|i - j| < 5$) constraints. In addition, four hydrogen bonds (Lys-1–Arg-5, Leu-2–His-6, Phe-3–Leu-7 and Lys-4–Lys-8) could be identified by inspection of

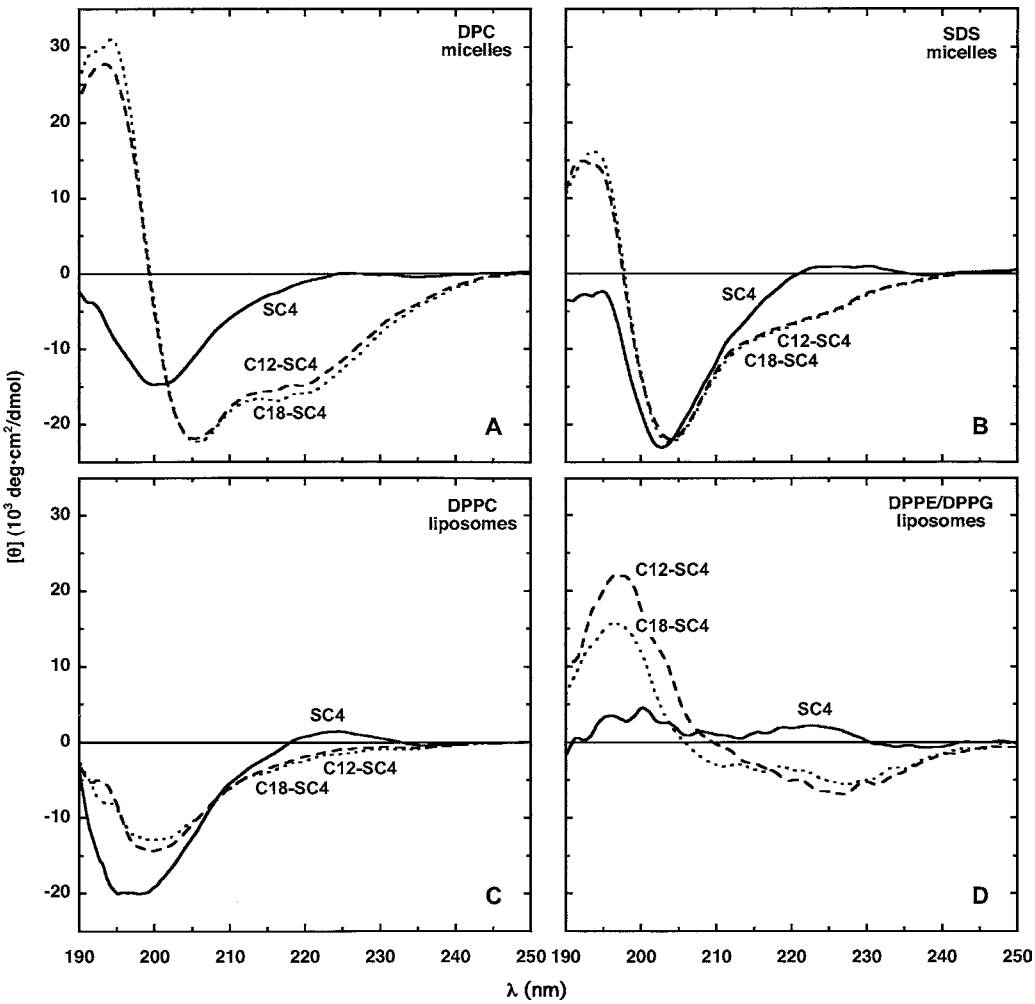

Figure 3 CD spectra of SC4 (unbroken lines), C12-SC4 (dashed lines) and C18-SC4 (dotted lines) in micelle and liposome membrane mimics

In micellar mimics, the SC4 amphiphiles showed spectra consistent with helical conformation in DPC (**A**) and somewhat less helix in SDS (**B**). Liposome membrane mimics showed spectra indicating little SC4 amphiphile structure in DPPC (**C**), the erythrocyte mimic, but a more structured state in bacterial-mimicking DPPE/DPPG liposomes (**D**). The SC4 peptide spectra indicate little structure under any condition. Spectra in water looked similar to those in DPPC liposomes; results at 37 °C were similar for all conditions.

initial C12-SC4 structures and from NH temperature coefficients, giving rise to eight hydrogen-bond-distance constraints. The total number of experimentally derived constraints was therefore 204, an average of 17 constraints per residue. One hundred structures were calculated using NOE and H-bond constraints; 24 final structures with no NOE violations greater than 0.5 Å were obtained (Figure 7A). Structural statistics (Table 2) show that the structures satisfy experimental constraints well. Together, the above data indicate that the structures used to represent the solution conformation of C12-SC4 are well converged. The average root-mean-square deviation for backbone heavy atoms of α-helical residues was 0.24 Å, for all backbone heavy atoms was 0.80 Å, and for the entire molecule (excluding the fatty acid tail) was 1.453 Å. The NMR structure of C12-SC4 in DPC micelles showed an amphipathic, α-helical conformation over much of the length of the peptide (Figures 7B and 7C).

Membrane interactions assessed by tryptophan fluorescence spectroscopy

We used tryptophan fluorescence spectroscopy to probe the environment of the Trp-9 residue of the SC4 molecules in water, liposomes and micelles (Table 3). The emission maximum for SC4, C12-SC4 and C18-SC4 in water was approx. 354 nm. A blue shift from this maximum suggests that the tryptophan is in a more hydrophobic environment [38]. In DPPC liposomes (eukaryotic membrane mimic), the position of the emission maximum did not change for SC4, but the maxima for C12-SC4 and C18-SC4 were slightly blue shifted. In DPPE/DPPG liposomes (bacterial membrane mimic), the emission maxima showed strong blue shifts for all three molecules, with the magnitude of the shift being larger for either SC4 amphiphile than for the SC4 peptide. Similar results were obtained at 37 °C, the temperature at which bactericidal assays were performed. In DPC or SDS micellar environments, the Trp-9 emission peak was blue-shifted and at levels comparable with those observed in DPPE/DPPG liposomes. This suggests that our NMR structural studies in DPC micelles probably reflect the environment of the C12-SC4 amphiphile in bacterial membranes.

Membrane interactions assessed by NMR chemical shifts

While αH and NH chemical shift differences generally reflect α-helix or β-sheet structure and stability [37], side-chain chemical

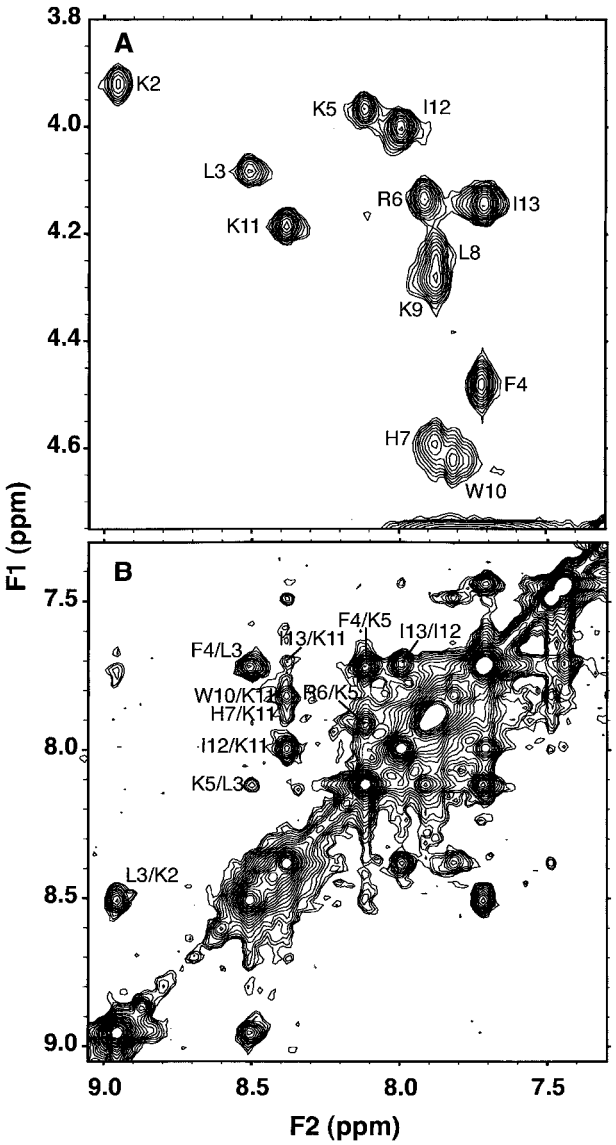

Figure 4 Regions of TOCSY (A) and NOESY (B) spectra for C12-SC4 in DPC micelles

The dispersion of the TOCSY spectrum and long-range NOEs indicate a structured state for C12-SC4 in DPC micelles.

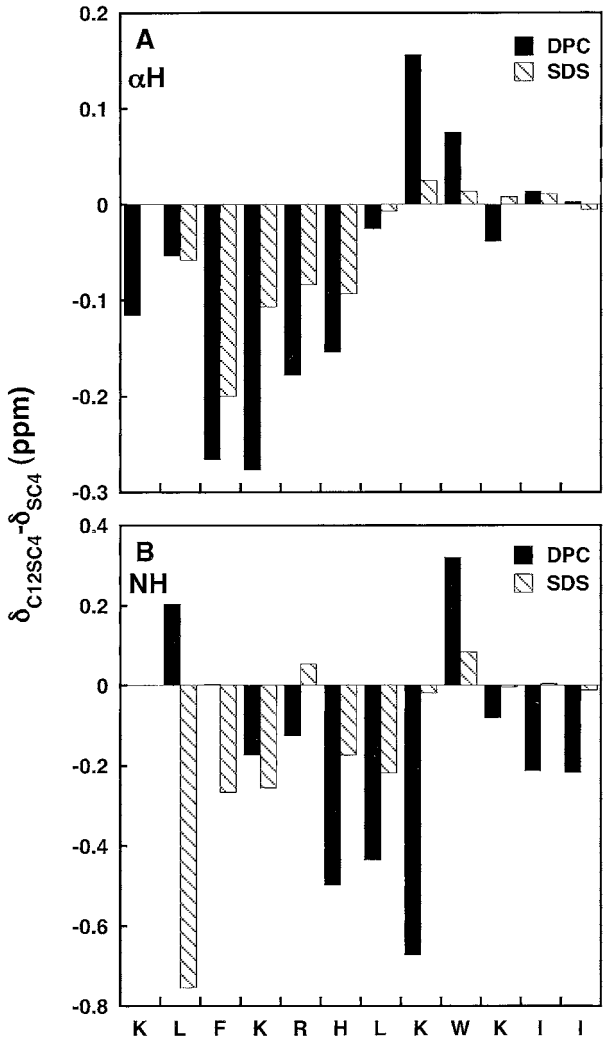

Figure 5 αH (A) and NH (B) chemical shifts for C12-SC4 in DPC or SDS relative to SC4 under the same conditions

The upfield nature of the shifts indicates stabilization of helical conformation, especially in residues Lys-1–His-7, as a result of fatty acid conjugation.

shifts can provide insight into the environment with which the folded peptide is interacting. This can be particularly insightful when shift differences other than βCH2 groups in longer side-chains are large.

We compared the side-chain chemical shifts for C12-SC4 in micelles (DPC or SDS) with those of the SC4 peptide under the same conditions (Figure 8); this comparison examines the effect of adding the fatty acid tail to the SC4 peptide. Note that this 'shift difference' is different from the standard use of the chemical shift index [37]. The shift differences associated with γCH and δCH groups are relatively large in the longer side-chain-containing amino acid residues, even compared with their αH, βCH and NH groups (compare with Figure 5). This indicates that the environment around the side-chains is being significantly perturbed by the presence of the fatty acid tail, probably a combination of conformation change and increased interaction with the detergent micelles. Side-chain chemical shift differences tended to be larger for C12-SC4 in SDS than in DPC. In DPC, the largest chemical shift difference was observed for Lys-4 and Lys-8; shift differences in SDS were also larger for these two residues. The larger shift difference for the C-terminal Ile-11 and Ile-12 residues may indicate a more micelle-buried environment for the terminus of the peptide in DPC. In SDS, large shifts were also found for Lys-1, Phe-3 and Lys-10. The large shift differences of the lysine side-chains in SDS suggest that interactions are primarily between the peptide lysines and the surface negative charges on the SDS micelles. This is also consistent with the smaller shift differences observed for other residues in the peptide.

An interaction between lysine side-chains and the SDS micelle surface is also supported by the observation of TOCSY αH, βH, γH and δH proton cross-peaks from terminal side-chain amines of the four C12-SC4 lysine residues in SDS micelles (Figure 9). The observation of lysine εNH_3^+ resonances from the peptide in the presence of SDS micelles indicates that εNH protons do not readily exchange with water. Although this could occur if the peptide were buried within an environment of low dielectric, i.e. within the micelle, the more likely explanation, especially

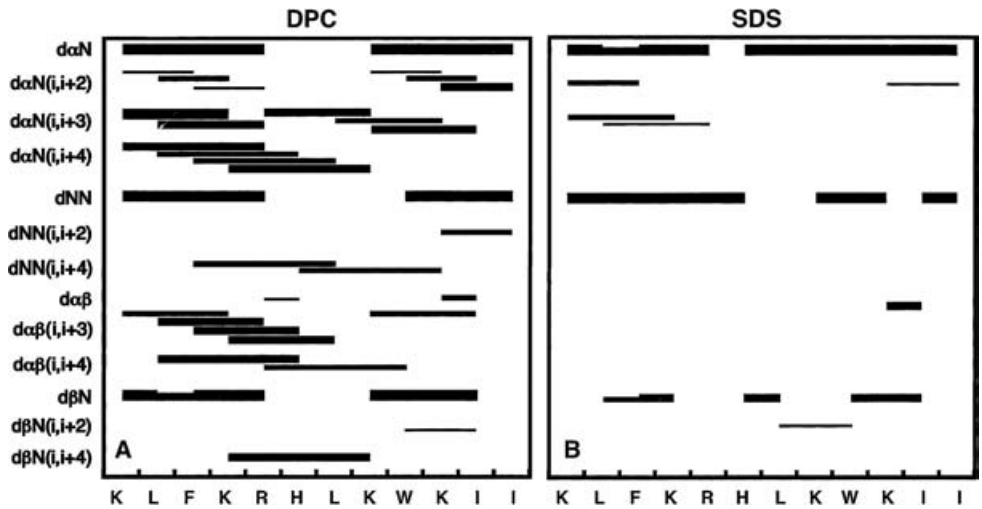

Figure 6 NOE connectivity for C12-SC4 in (A) DPC and (B) SDS micelles

The number and regularity of NOE connectivities in DPC suggests an ordered state, and the patterns are consistent with an α-helical conformation in residues Lys-1 through Lys-8. In SDS, there were far fewer observable NOEs, although several of them are consistent with a somewhat structured peptide.

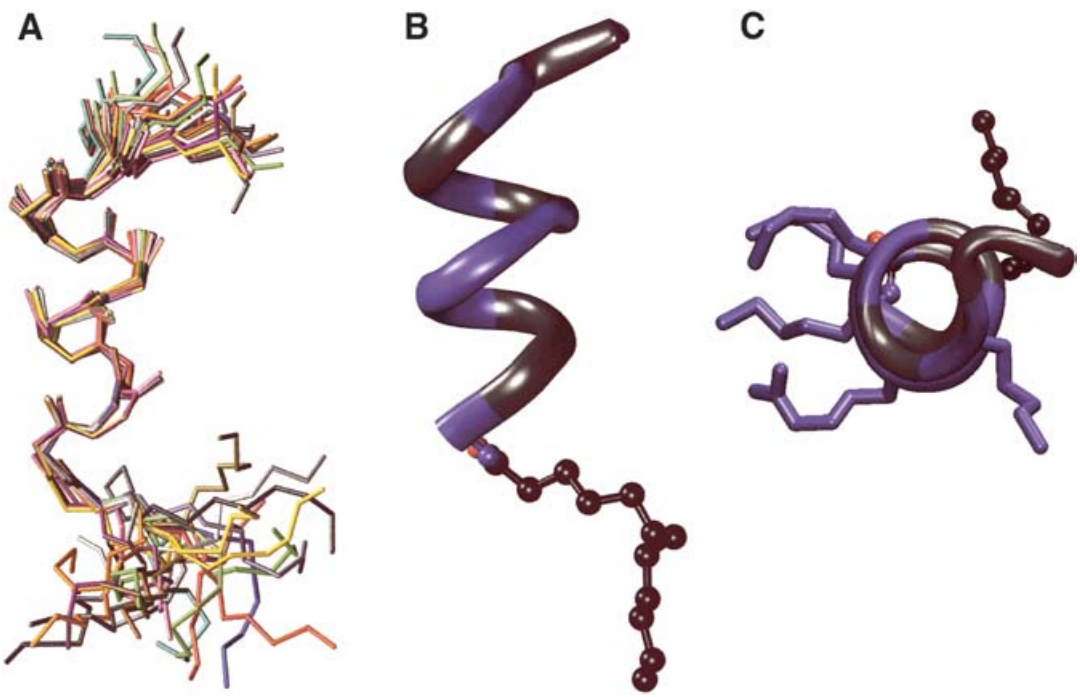

Figure 7 NOE-derived structures of C12-SC4 in DPC micelles

(**A**) Superposition of the 24 final structures, using residues Lys-1 through Trp-9 for alignment. (**B**) A ribbon backbone representation of one structure, showing the overall helical fold and a less-ordered C-terminus. Polar residues are shown in blue and apolar residues in grey. The fatty acid tail is shown as ball-and-stick model. (**C**) An axial view of the average structure, demonstrating the distribution of charged side chains (arginine and lysine) in an amphipathic helix. The colours are as described in (**B**).

considering that the cross-peaks are not observed in DPC micelles, is that this effect is the result of electrostatic interactions with the micelle surface.

DISCUSSION

Fatty acid conjugation of the SC4 peptide, itself potently antibacterial, creates an even more potent bactericidal agent and broadens the range of susceptible bacteria to include drug-resistant, Gram-positive and anthrax strains. Conjugation of fatty acids to SC4 increased bactericidal activity most dramatically against Gram-positive bacteria, increasing the activity of SC4 up to 30-fold (Figure 2 and Table 1). Moreover, drug-resistant Gram-positive strains that are susceptible only to the conventional antibiotic vancomycin were effectively killed at sub-micromolar concentrations of SC4 peptide-amphiphiles. This is particularly noteworthy, because of the difficulty in developing antibiotics that can combat drug-resistant strains in the clinic.

Table 2 Structural statistics of NOE-derived C12-SC4 structures

None of the 24 final structures exhibited distance restraint violations greater than 0.5 Å. Values are expressed as the means ± S.D. RMSD, root-mean-square deviation.

Parameter	RMSD	Energy (J/mol)
NOE	0.1666 ± 0.0039 Å	117.96 ± 5.53
Angles	0.9334 ± 0.0218°	71.56 ± 3.37
Bonds	0.0085 ± 0.0002 Å	21.01 ± 1.06
Impropers	0.7675 ± 0.0619°	13.54 ± 2.03
Total*	1.453 Å	255.40 ± 6.42

* Total RMSD was calculated for heavy atoms and does not include the fatty acid tail.

Table 3 Tryptophan fluorescence emission maxima in water and membrane-mimicking environments

Emission spectra were collected from 300–450 nm; excitation was at 280 nm; at 25 °C; concentration = 5 μM. Values are peak position (nm) means ± S.D., $n = 3$. Peptide/lipid ratios: DPPC and DPPE/DPPG, 1:20; DPC, 1:500; SDS, 1:1000.

	Peak position (nm)				
Peptide	Water	DPPC*	DPPE/DPPG	DPC†	SDS†
SC4	352.7 ± 0.6	353.3 ± 1.2	342.0 ± 0.0	342	341
C12-SC4	353.0 ± 1.0	348.7 ± 2.1	338.0 ± 0.0	344	341
C18-SC4	353.3 ± 1.2	349.0 ± 1.7	339.7 ± 3.2	344	342

† $n = 1$.

Our results suggest that fatty acid conjugation to the peptide elicits three effects: (1) increases bactericidal activity, (2) increases membrane affinity and (3) stabilizes secondary structure in a membrane environment. Although previous work has suggested an optimal tail length of 11 or 12 carbon atoms [17–21], we find that an 18-carbon acyl chain is more effective than a 12-carbon tail against Gram-positive bacteria. Although we cannot absolutely link structural stability due to the presence of the acyl chain with bactericidal efficacy, the results suggest such a connection. Peptide-amphiphiles have been shown to stabilize a variety of α-helical and triple-helical structures in peptides that are otherwise unstructured [24,39], a process that appears to be mediated through self-assembly or incorporation into micelles or liposomes [23]. The development of α-helical structure upon interacting with membranes is an important step in the activity of antibacterial peptides [40], and factors that stabilize helical structure in membrane-bound peptides may therefore assist in developing the amphipathicity apparently required for lysis of the bacterial membrane. On the other hand, peptides that assemble in solution prior to interacting with the membrane have shown reduced antibacterial potency [41]. Although we have observed assembly of SC4 amphiphiles in solution, such aggregation occurred only well above biologically relevant concentrations. C12-SC4 and C18-SC4 form aggregates only at concentrations above approx. 0.5 mM to 5 mM (results not shown), levels more than 100-times higher than those used in either our biological assays or our biophysical experiments. It is possible, however, that the tendency of SC4 amphiphiles to self-aggregate may play a role in permeabilizing cell membranes by allowing membrane-bound amphiphiles to aggregate within the membrane at surface concentrations below that required for the SC4 peptide.

Structural details of the C12-SC4 headgroup are likely to be as important as the conformational stabilization imparted by the presence of the tail. We expect that our NMR results in DPC

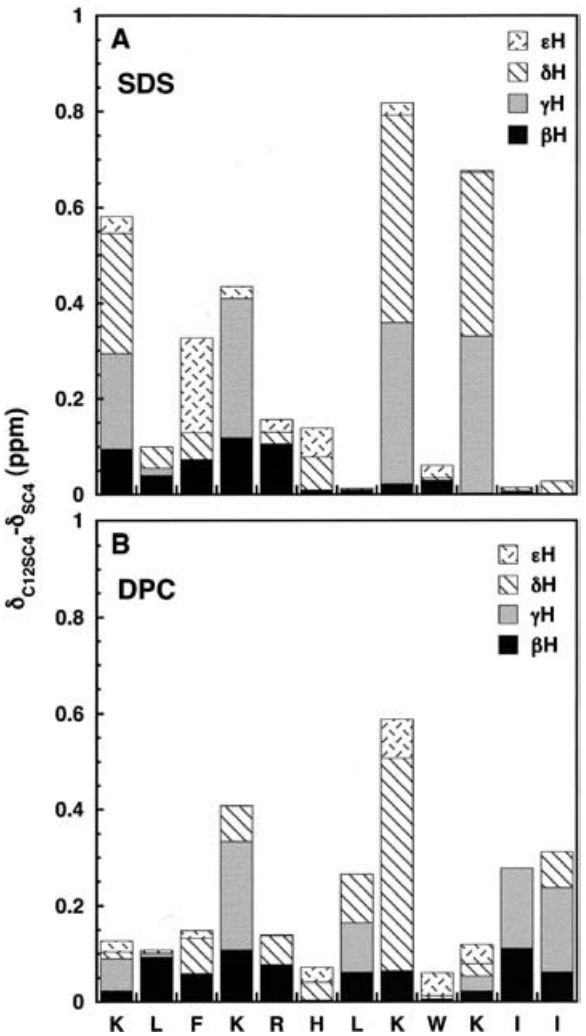

Figure 8 Side chain chemical shift differences between C12-SC4 in SDS (A) and DPC (B) micelles and SC4 peptide under the same conditions

All chemical shift differences are given as absolute values to avoid speculation into reasons for positive and negative values.

are likely to be well correlated with the behaviour of C12-SC4 in bacterial membranes, based on the similarity of blue shifts observed in tryptophan fluorescence spectra under each condition (Table 3). NMR structural models of C12-SC4 in DPC micelles reveal some of the details of why these molecules are such potent antibacterial agents (Figure 7). The helical secondary structure formed by the peptide shows clear amphipathic character, with a large cationic face and a smaller hydrophobic face on the opposite side of the helix. A large angle subtended by the cationic face of the helix has been shown in model systems to lead to high bactericidal potency relative to peptides with a smaller cationic face [42]. It should also be mentioned that the NMR structure of C12-SC4 in DPC micelles is similar to that reported by Mayo et al. [25] for the free SC4 peptide in TFE/water. Although the similarity of these helical structures of the SC4 peptide in two membrane-mimicking media is not surprising, the observation of reduced chemical shift dispersion and the attenuation of long-range NOEs for the free SC4 peptide in DPC micelles indicates less stable helical structure in the absence of the acyl chain. This suggests that interaction of the acyl chain in the micelles imparts a more stable helix conformation to the peptide-amphiphile.

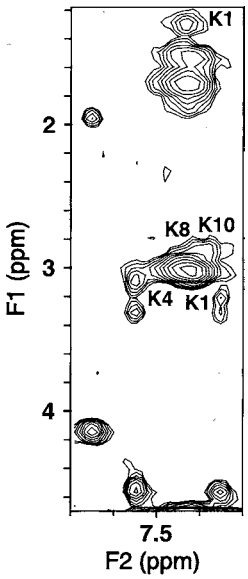

Figure 9 Lysine side-chain amine region of TOCSY spectra for C12-SC4 in SDS micelles

No TOCSY cross-peaks were observed in this region for C12-SC4 in DPC micelles.

The non-specific increase in membrane affinity of C12-SC4 and C18-SC4 is also likely to play a role in bactericidal activity. Recalling that DPPE/DPPG liposomes mimic bacterial membranes, and DPPC liposomes mimic erythrocyte membranes, it is easy to draw parallels between our tryptophan fluorescence spectra for SC4 and its amphiphiles and our biological assays with the same molecules. The general increase in SC4 bactericidal activity upon fatty acid conjugation (Table 1) is reflected in the more hydrophobic environment of the tryptophan in C12-SC4 and C18-SC4 in DPPE/DPPG and DPPC liposomes respectively (Table 3). The enhanced membrane affinity of the SC4 peptide-amphiphiles (as displayed by their fluorescence spectra) would seem to explain, at least in part, the increased biological activity of the amphiphiles.

SC4 and C12-SC4 are known to permeabilize bacterial membranes; so it is logical to look towards models of membrane-permeabilizing peptides for insight into the mechanism of SC4 amphiphiles. The basic models used to describe the membrane-disrupting activity of amphipathic, α-helical antibacterial peptides (reviewed by Oren and Shai [26]) are: (1) the barrel-stave model in which transmembrane pores form via the aggregation of a small number of peptides spanning the bacterial membrane, (2) the carpet model in which a large number of peptides aggregate on and solubilize regions of the bacterial membrane in a detergent-like manner, and (3) the toroidal pore model, in which membrane-aggregated peptides lead to stable pores lined with lipids and peptides. Both the chemical shifts of C12-SC4 side chains (Figure 8) and the presence of TOCSY connectivity involving εNH protons (Figure 9) in SDS micelles support the idea of electrostatic interactions occurring between lysine side chains and the SDS micelle surface, which is consistent with the tenets of any of these models. The barrel-stave model, however, is an unlikely choice, if only for simple geometric considerations. The 12-residue SC4 helix is probably too short to span the bacterial membrane. Additionally, the charge on SC4 is $+5$, which modelling suggests is too high for formation of stable barrel-like pores [43]. Our observations are consistent with the toroidal pore model in which membrane pores are lined with a mixture of membrane lipids and peptides, with peptides not extending entirely through the membrane.

The presence of the fatty acid tail in SC4 peptide-amphiphiles may provide a means of increasing aggregation at the membrane surface, a two-dimensional analogue of the aggregation observed for SC4 peptide-amphiphiles in solution. In the context of the toroidal pore model, this increase in aggregation behaviour would allow for a decrease in the surface concentration required for membrane perforation relative to the SC4 peptide. This is consistent with increased bactericidal activity at lower concentrations for SC4 amphiphiles compared with SC4 peptide in Gram-positive organisms.

Conclusion

The results show increases of antibacterial activity of SC4 by conjugating C12 and C18 acyl chains: the activity is increased by approximately a factor of 30 on Gram-positive bacteria, but is not significantly increased on Gram-negative bacteria. The level of activity reached by C18-SC4 on Gram-positive strains becomes similar to that observed for unmodified SC4 on Gram-negative strains. The C18 acyl chain is thus responsible for better interaction of SC4 with the Gram-positive bacteria. SC4 alone does not appear to be able to penetrate the thick peptidoglycan layer in Gram-positive bacteria, whereas in Gram-negative bacteria it can reach the phospholipid bilayer. The presence of a fatty acid tail also increases the ability of the peptide to neutralize LPS endotoxin. Biophysical studies (CD, NMR and fluorescence spectroscopy) demonstrate that fatty acid conjugation enhances membrane affinity and helix formation in membrane-bound SC4 peptide-amphiphiles.

We thank Dinesha Walek at the University of Minnesota Microchemical Facility for her expertise in peptide synthesis, Dr Irina Nesmelova and Monica Arroyo for assistance in NMR structure analysis, Dr Ruud Dings for performing cytotoxicity assays, Dr Igor Negrashov for assistance with fluorescence measurements, David C. Tiemeier for suggesting experiments with drug-resistant bacterial strains and Dr Patrick Schlievert for providing drug-resistant bacteria. N.A.L. was supported by a Whitaker Foundation Graduate Fellowship. NMR instrumentation was provided with funds from the National Science Foundation (number BIR-961477), the University of Minnesota Medical School and the Minnesota Medical Foundation.

REFERENCES

1 Otvos, Jr, L. (2000) Antibacterial peptides isolated from insects. J. Pept. Sci. **6**, 497–511
2 Simmaco, M., Mignogna, G. and Barra, D. (1998) Antimicrobial peptides from amphibian skin: what do they tell us? Biopolymers **47**, 435–450
3 Ganz, T. (2001) Antimicrobial proteins and peptides in host defense. Semin. Respir. Infect. **16**, 4–10
4 Tossi, A. (2003) Antimicrobial Sequences Database. Department of Biochemistry, Biophysics, and Macromolecular Chemistry, University of Trieste, Trieste, Italy (http://www.bbcm.units.it/~tossi/pag1.htm)
5 Whitmore, L., Chugh, J., Snook, C. F. and Wallace, B. A. (2003) Peptaibol Database. School of Crystallography, Birkbeck College, University of London, London, U.K. (http://www.cryst.bbk.ac.uk/peptaibol/home.shtml)
6 Wade, D. and Englund, J. (2003) Synthetic Antibiotic Peptides Database. J. Haartman Institute and the National Library of Health Sciences, Helsinki University, Helsinki, Finland (http://oma.terkko.helsinki.fi:8080/~SAPD/)
7 Zasloff, M., Martin, B. and Chen, H. C. (1988) Antimicrobial activity of synthetic magainin peptides and several analogues. Proc. Natl. Acad. Sci. U.S.A. **85**, 910–913
8 Selsted, M. E. and Harwig, S. S. (1989) Determination of the disulfide array in the human defensin HNP-2. A covalently cyclized peptide. J. Biol. Chem. **264**, 4003–4007
9 Agerberth, B., Lee, J. Y., Bergman, T., Carlquist, M., Boman, H. G., Mutt, V. and Jornvall, H. (1991) Amino acid sequence of PR-39. Isolation from pig intestine of a new member of the family of proline-arginine-rich antibacterial peptides. Eur. J. Biochem. **202**, 849–854
10 Selsted, M. E., Novotny, M. J., Morris, W. L., Tang, Y. Q., Smith, W. and Cullor, J. S. (1992) Indolicidin, a novel bactericidal tridecapeptide amide from neutrophils. J. Biol. Chem. **267**, 4292–4295

11 Tsubery, H., Ofek, I., Cohen, S. and Fridkin, M. (2001) N-terminal modifications of Polymyxin B nonapeptide and their effect on antibacterial activity. Peptides **22**, 1675–1681

12 Toniolo, C., Crisma, M., Formaggio, F., Peggion, C., Monaco, V., Goulard, C., Rebuffat, S. and Bodo, B. (1996) Effect of N-acyl chain length on the membrane-modifying properties of synthetic analogs of the lipopeptaibol trichogin GA IV. J. Am. Chem. Soc. **118**, 4952–4958

13 Giangaspero, A., Sandri, L. and Tossi, A. (2001) Amphipathic alpha helical antimicrobial peptides. Eur. J. Biochem. **268**, 5589–5600

14 Matsuzaki, K., Yoneyama, S., Fujii, N., Miyajima, K., Yamada, K., Kirino, Y. and Anzai, K. (1997) Membrane permeabilization mechanisms of a cyclic antimicrobial peptide, tachyplesin I, and its linear analog. Biochemistry **36**, 9799–9806

15 Andreu, D., Merrifield, R. B., Steiner, H. and Boman, H. G. (1985) N-terminal analogues of cecropin A: synthesis, antibacterial activity, and conformational properties. Biochemistry **24**, 1683–1688

16 Shafer, W. M., Pohl, J., Onunka, V. C., Bangalore, N. and Travis, J. (1991) Human lysosomal cathepsin G and granzyme B share a functionally conserved broad spectrum antibacterial peptide. J. Biol. Chem. **266**, 112–116

17 Mak, P., Pohl, J., Dubin, A., Reed, M. S., Bowers, S. E., Fallon, M. T. and Shafer, W. M. (2003) The increased bactericidal activity of a fatty acid-modified synthetic antimicrobial peptide of human cathepsin G correlates with its enhanced capacity to interact with model membranes. Int. J. Antimicrob. Agents **21**, 13–19

18 Wakabayashi, H., Matsumoto, H., Hashimoto, K., Teraguchi, S., Takase, M. and Hayasawa, H. (1999) N-Acylated and D enantiomer derivatives of a nonamer core peptide of lactoferricin B showing improved antimicrobial activity. Antimicrob. Agents Chemother. **43**, 1267–1269

19 Majerle, A., Kidric, J. and Jerala, R. (2003) Enhancement of antibacterial and lipopolysaccharide binding activities of a human lactoferrin peptide fragment by the addition of acyl chain. J. Antimicrob. Chemother. **51**, 1159–1165

20 Avrahami, D. and Shai, Y. (2002) Conjugation of a magainin analogue with lipophilic acids controls hydrophobicity, solution assembly, and cell selectivity. Biochemistry **41**, 2254–2263

21 Chicharro, C., Granata, C., Lozano, R., Andreu, D. and Rivas, L. (2001) N-terminal fatty acid substitution increases the leishmanicidal activity of CA(1-7)M(2-9), a cecropin-melittin hybrid peptide. Antimicrob. Agents Chemother. **45**, 2441–2449

22 Berndt, P., Fields, G. B. and Tirrell, M. (1995) Synthetic lipidation of peptides and amino acids: monolayer structure and properties. J. Am. Chem. Soc. **117**, 9515–9522

23 Gore, T., Dori, Y., Talmon, Y., Tirrell, M. and Bianco-Peled, H. (2001) Self-assembly of model collagen peptide amphiphiles. Langmuir **17**, 5352–5360

24 Yu, Y. C., Tirrell, M. and Fields, G. B. (1998) Minimal lipidation stabilizes protein-like molecular architecture. J. Am. Chem. Soc. **120**, 9979–9987

25 Mayo, K. H., Haseman, J., Young, H. C. and Mayo, J. W. (2000) Structure-function relationships in novel peptide dodecamers with broad-spectrum bactericidal and endotoxin-neutralizing activities. Biochem. J. **349**, 717–728

26 Oren, Z. and Shai, Y. (1998) Mode of action of linear amphipathic α-helical antimicrobial peptides. Biopolymers **47**, 451–463

27 Johnson, J. R. and Brown, J. J. (1996) A novel multiply primed polymerase chain reaction assay for identification of variant papG genes encoding the Gal(α1-4)Gal-binding PapG adhesins of *Escherichia coli*. J. Infect. Dis. **173**, 920–926

28 Bohach, G. A., Kreiswirth, B. N., Novick, R. P. and Schlievert, P. M. (1989) Analysis of toxic shock syndrome isolates producing staphylococcal enterotoxins B and C1 with use of southern hybridization and immunologic assays. Rev. Infect. Dis. **11**, S75–S82

29 Schlievert, P. M. and Blomster, D. A. (1983) Production of staphylococcal pyrogenic exotoxin type C: influence of physical and chemical factors. J. Infect. Dis. **147**, 236–242

30 Reference deleted.

31 Young, N. S., Levin, J. and Prendergast, R. A. (1972) An invertebrate coagulation system activated by endotoxin: evidence for enzymatic mediation. J. Clin. Invest. **51**, 1790–1797

32 Adler, A. J., Greenfield, N. J. and Fasman, G. D. (1973) Circular dichroism and optical rotary dispersion of proteins and polypeptides. Methods Enzymol. **27**, 675–735

33 Greenfield, N. and Fasman, G. D. (1969) Computed circular dichroism spectra for the evaluation of protein conformation. Biochemistry **8**, 4108–4116

34 Delaglio, F., Grzesiek, S., Viuster, G. W., Zhu, G., Pfeifer, J. and Bax, A. (1995) NMRPipe: a multidimensional spectral processing system based on UNIX pipes. J. Biomol. NMR **6**, 277–293

35 Nilges, M., Kuszewski, J. and Brunger, A. T. (1991) Computational Aspects of the Study of Biological Macromolecules by NMR, Plenum Press, New York

36 Humphrey, W., Dalke, A. and Schulten, K. (1996) VMD – visual molecular dynamics. J. Mol. Graphics **14**, 33–38

37 Wishart, D. S., Sykes, B. D. and Richards, F. M. (1992) The chemical shift index: a fast and simple method for the assignment of protein secondary structure through NMR spectroscopy. Biochemistry **31**, 1647–1651

38 Lakowicz, J. (1983) Principles of Fluorescence Spectroscopy, Plenum Press, New York

39 Fields, G. B., Lauer, J. L., Dori, Y., Forns, P., Yu, Y. C. and Tirrell, M. (1998) Protein-like molecular architecture: biomaterial applications for inducing cellular receptor binding and signal transduction. Biopolymers **47**, 143–151

40 Bechinger, B., Zasloff, M. and Opella, S. J. (1993) Structure and orientation of the antibiotic peptide magainin in membranes by solid-state nuclear magnetic resonance spectroscopy. Protein Sci. **2**, 2077–2084

41 Houston, Jr, M. E., Kondejewski, L. H., Karunaratne, D. N., Gough, M., Fidai, S., Hodges, R. S. and Hancock, R. E. (1998) Influence of preformed α-helix and α-helix induction on the activity of cationic antimicrobial peptides. J. Pept. Res. **52**, 81–88

42 Wieprecht, T., Dathe, M., Epand, R. M., Beyermann, M., Krause, E., Maloy, W. L., MacDonald, D. L. and Bienert, M. (1997) Influence of the angle subtended by the positively charged helix face on the membrane activity of amphipathic, antibacterial peptides. Biochemistry **36**, 12869–12880

43 Zemel, A., Fattal, D. R. and Ben-Shaul, A. (2003) Energetics and self-assembly of amphipathic peptide pores in lipid membranes. Biophys. J. **84**, 2242–2255

Received 12 September 2003/6 November 2003; accepted 10 November 2003
Published as BJ Immediate Publication 10 November 2003, DOI 10.1042/BJ20031393